Scaling of the transport properties in the $Y_{1-y}Pr_yBa_2Cu_3O_x$ system

J. Vanacken, L. Trappeniers, P. Wagner, L. Weckhuysen, V. V. Moshchalkov, and Y. Bruynseraede
Laboratorium voor Vaste-Stoffysica en Magnetisme, Katholieke Universiteit Leuven, Celestijnenlaan 200 D, B-3001 Heverlee, Belgium
(Received 22 June 2001; published 22 October 2001)

We report on the temperature dependent resistivity of $YBa_2Cu_3O_x$ and $(Y_{0.6}Pr_{0.4})Ba_2Cu_3O_x$ epitaxial thin films, measured in pulsed magnetic fields up to 50 T. The zero-field $\rho(T)$ data for various levels of hole doping p can be scaled onto one single universal curve by using a linear transformation of both temperature and resistivity. This universal curve exhibits a linear $\rho(T)$ at high temperatures $T>T^*$ (region I) and a superlinear $\rho(T)$ at intermediate temperatures $T_{MI}<T<T^*$ (region II). The ground state in the low temperature region $T<T_{MI}$ (region III) is masked by the presence of superconductivity below T_c, but is accessible in high magnetic fields. The high field measurements reveal that $YBa_2Cu_3O_x$ (for $x<6.8$) and $(Y_{0.6}Pr_{0.4})Ba_2Cu_3O_x$ (for all levels of oxygen content) have an ''insulatinglike'' ground state at low temperatures and that the universal scaling may be extended to region III. The existence of a universal $\rho(T)$ curve indicates that the same mechanisms are dominating the scattering of the charge carriers in these materials but with a different energy scale depending on the carrier concentration and/or the defect structure.

DOI: 10.1103/PhysRevB.64.184425 PACS number(s): 74.25.Fy, 74.20.Mn, 74.62.Dh

I. INTRODUCTION

Although the transport properties of the underdoped cuprates are widely studied, the different scattering mechanisms in these materials are still not clearly revealed. The temperature dependence of the zero-field normal-state resistivity $\rho(T)$ for $YBa_2Cu_3O_x$ with various oxygen doping levels exhibits an almost perfect scaling behavior both in temperature and resisitivity.[1] At low temperatures, the presence of superconductivity made the observation of the normal state transport properties impossible. The normal-state resistivity, however, can in a natural way be extended to the region below the critical temperature T_c by suppressing the ''unwanted'' superconducting phase by the use of strong magnetic fields. In this way, Ando and co-workers have found a logarithmic diverging $\rho(T)\sim\ln(1/T)$ normal state in $La_{2-x}Sr_xCuO_4$ (Refs. 2–4) and $Bi_2Sr_2CuO_y$ (Refs. 5–8) cuprates at low temperatures.

In this work we will address the question if the scaling in the Y-Ba-Cu-O system persists into the low temperature area. To study the transport properties and their scaling in the whole temperature range, we have chosen ''123''-epitaxial thin films in which we systematically changed the hole content by varying the oxygen concentration x ($YBa_2Cu_3O_x$) and/or chemically substituting Y by Pr ($Y_{0.6}Pr_{0.4}Ba_2Cu_3O_x$).

Section II will describe the sample preparation method and the high field magnetotransport measuring technique. Section III reports on the temperature dependence of the resistivity in zero field. The magneto-resistivity is presented in Sec. IV. The temperature dependencies are completed with the high field data in Sec. V. Section VI, finally, addresses the extension of the scaling for these high field data.

II. EXPERIMENTAL METHOD

The as-grown films are prepared by dc magnetron sputtering from stoichiometric targets.[9] To achieve the desired oxygen content, the films are post annealed in a controlled oxygen partial pressure P_{O2}. This procedure is based on the knowledge of the (P_{O2}-T) phase diagram for fixed stable oxygen content x. The method has been proven reliable, and is discussed in detail in Ref. 10. The exact oxygen concentration of the films is not measured directly, but evaluated from the well documented $T_c(x)$ behavior.[10]

The magnetoresistance and Hall effect measurements were performed in the pulsed fields facility of the K.U. Leuven[11,12] by using a homemade flow-cryostat and 50 T coil. All data reported in this work were obtained on thin films, patterned (1000×50 μm strip) for four probe measurements in the transverse geometry ($H\perp I$) with the magnetic field perpendicular to the film ($H\|c$) and the current sent along the ab plane ($I\|ab$). The main physical properties are summarized in Table I.

III. ZERO-FIELD RESISTIVITY

The temperature dependence of the resistivity $\rho(T)$ for the $YBa_2Cu_3O_x$ and $(Y_{0.6}Pr_{0.4})Ba_2Cu_3O_x$ thin films is shown in Fig. 1. At optimal doping ($YBa_2Cu_3O_{6.95}$), $\rho(T)$ is linear down to just above the critical temperature T_c. At lower doping levels, the regime of linear $\rho(T)$ shifts to higher temperatures and an S-shape, superlinear, behavior emerges between T_c and T^* [T^* is commonly used to denote the temperature at which the linear $\rho(T)$ transforms into the superlinear behavior]. The reduced resistivity in region $T<T^*$ is accompanied by an increase of the slope in the linear $\rho(T)$ region and an overall increase of the resistivity (both $\rho_{290\,K}$ and the residual resistance ρ_0, see Table I). The strong increase of ρ_0 is an indication that reducing the oxygen content or substituting Pr for Y, apart from lowering the charge carrier density, also induces an appreciable disorder. In Pr-doped $YBa_2Cu_3O_x$, there are at least two effects playing a significant role: hole-filling changes in the density of charge carriers and magnetic scattering by the paramagnetic Pr ions. The observed changes in the behavior of $\rho(T)$ for $YBa_2Cu_3O_x$, and $Y_{1-z}Pr_zBa_2Cu_3O_x$ are well documented in the literature for both thin films and single crystals.[1,13–17] An ''insulatinglike'' $\rho(T)$ behavior can coexist with the super-

TABLE I. Overview of the $YBa_2Cu_3O_x$ and $Y_{0.6}Pr_{0.4}Ba_2Cu_3O_x$ thin films. The oxygen content x, film thickness t, critical temperature T_c, width of the transition ΔT_c, residual resistivity ρ_0, resistivity at $T=290$ K, $\rho_{290\,K}$ and the ratio $\rho_{290\,K}/\rho_0$ as well as the scaling parameter Δ and the crossover temperature T^* are shown; $k_F l_0 = hc_0/e^2\rho_0$ values, with c_0 the average lattice constant in the c direction, are added for completeness.

x	t (Å)	$T_{c,\mathrm{mid}}$ (K)	ΔT_c (K)	ρ_0 ($\mu\Omega$ cm)	$\rho_{290\,K}$ ($\mu\Omega$ cm)	$k_F l_0$	$\rho_{290\,K}/\rho_0$	Δ (K)	T^* (K)
				$YBa_2Cu_3O_x$					
6.95	1770	92.2	1.1	48	579	7.8	~12	86.5	173
6.7	1770	58.2	2.7	209	1171	1.8	~5.6	174.3	349
6.45	1770	41.7	7.7	607	2237	0.6	~3.7	215.1	430
				$(Y_{0.6}Pr_{0.4})Ba_2Cu_3O_x$					
6.95	850	41.4	5.3	278	658	1.3	~2.4	158.7	317
6.85	850	31.8	6.7	459	1205	0.8	~2.6	185.9	372
6.7	850	22.3	12.7	805	1904	0.5	~2.4	184.5	369

conducting transition itself and T_c is closely correlated with the hole doping (e.g., the oxygen content or the level of Y/Pr substitution).

The linear $\rho(T)$ at temperatures above T^*, the superlinear $\rho(T)$ behavior below T^* and the saturating or increasing $\rho(T)$ at low temperatures are distinct features. The first and second feature are *universal* for all the curves reported in Figs. 1(a) and 1(b). This observation was the motivation to make a successful scaling analysis of the transport properties of $YBa_2Cu_3O_x$.[1] In Fig. 2(a) the scaled $\rho(T)$ curve is plotted for the $YBa_2Cu_3O_x$ thin films for which the temperature is rescaled with a parameter Δ and the resistivity plotted as $(\rho-\rho_0)/(\rho_\Delta-\rho_0)$, where ρ_Δ is the resistivity at $T=\Delta$. The parameter Δ defines the energy scale controlling the linear and superlinear behavior.

An interesting observation from these rescaled $\rho(T)$ data is that, although the $(Y_{0.6}Pr_{0.4})Ba_2Cu_3O_x$ and the $YBa_2Cu_3O_x$ data fall on the same universal curve, the energy scale Δ in the two systems differs substantially (see Table I). For the same oxygen content, the scaling parameter Δ is significantly higher in case of the $(Y_{0.6}Pr_{0.4})Ba_2Cu_3O_x$ films, although the critical temperature is about a factor of 2 lower. This apparent higher energy scale Δ for the $(Y_{0.6}Pr_{0.4})Ba_2Cu_3O_x$ system is further illustrated by the rescaled $\rho(T)$ data in Fig. 2(b) for which the linear regime is only reached at room temperature. For the $YBa_2Cu_3O_x$ system the linear regime is easily obtained for the sample with the highest oxygen content.

The temperature T^*—crossover temperature from linear

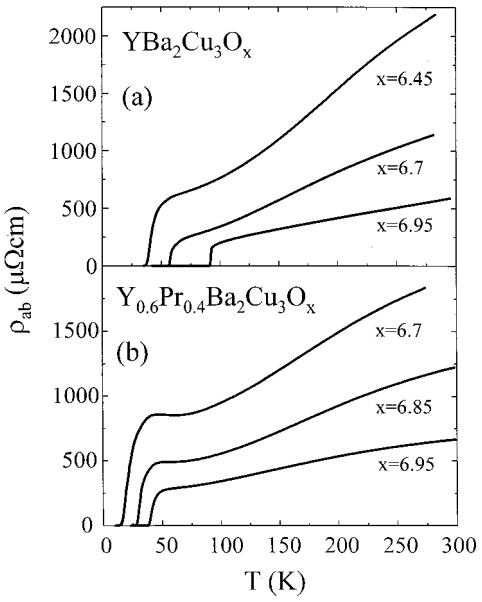

FIG. 1. The zero-field resistivity $\rho(T)$ for the $YBa_2Cu_3O_x$ (a) and the $(Y_{0.6}Pr_{0.4})Ba_2Cu_3O_x$ (b) thin films.

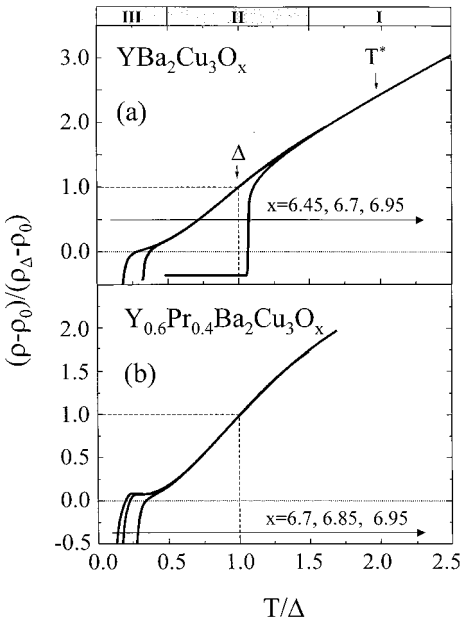

FIG. 2. Scaling of the zero-field $\rho(T)$ data for the $YBa_2Cu_3O_x$ (a) and $(Y_{0.6}Pr_{0.4})Ba_2Cu_3O_x$ (b) thin films with different oxygen contents x. The temperature is rescaled with Δ (an energy scale) and the resistivity is given by $(\rho-\rho_0)/(\rho_\Delta-\rho_0)$ in which the residual resistivity ρ_0 is subtracted and ρ_Δ is the resistivity at $T=\Delta$. Three regions of different $\rho(T)$ behavior are indicated together with the energy scale Δ and the crossover temperature T^*.

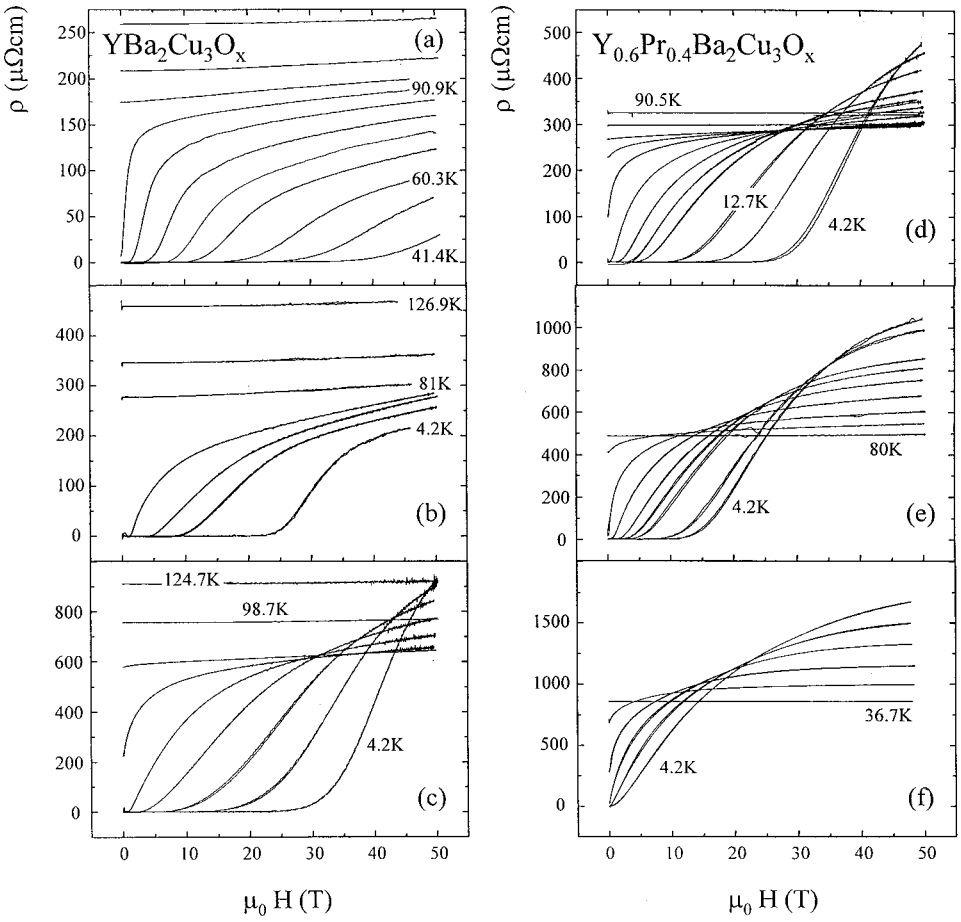

FIG. 3. Field dependence of the in-plane resistivity $\rho_{ab}(H)$ for an epitaxial $YBa_2Cu_3O_x$ film with $x=6.95$ (a), $x=6.7$ (b), and $x=6.45$ (c) as well as for an epitaxial $Y_{0.6}Pr_{0.4}Ba_2Cu_3O_x$ film with $x=6.95$ (d), $x=6.85$ (e), $x=6.7$ (f). The field H was applied $H\|c$ and the current $I\|ab$.

to S-shaped—is approximately equal to 2Δ, the energy scale of the conduction process (see Table I). The T^* increases as the doping level is reduced. These general observations are valid for both the $YBa_2Cu_3O_x$ and the $(Y_{0.6}Pr_{0.4})Ba_2Cu_3O_x$ system and the region of linear $\rho(T)$ is labeled I in Fig. 2.

At lower temperatures $T<T^*$, the $\rho(T)$ curves deviate from linearity and a superlinear $\rho(T)$ behavior sets in. Although already observed in the individual $\rho(T)$ curves, our scaling analysis implies this enhanced conductivity (or reduced scattering) to be a universal feature of the conduction in the high-T_c samples. This region is labeled II in Fig. 2. The increased conductivity is often explained[18] by the opening of a pseudo-spin-gap below T^* (for a review see Ref. 19) and for that reason we have adopted this nomenclature. *The implications of our scaling analysis, however, are by far more general and are not restricted to any specific theoretical model* used to introduce T^*.

At low temperatures $T<0.25\Delta$ for $YBa_2Cu_3O_x$ and $T<0.35\Delta$ for the $(Y_{0.6}Pr_{0.4})Ba_2Cu_3O_x$ system, a saturation of the $\rho(T)$ curves is seen, with a small increase of ρ for the samples with the lowest oxygen concentration. This is the onset of a regime III, were the $\rho(T)$ curves have a negative slope $d\rho/dT$ and which might be associated with the onset of localization.

From the scaling, presented in Fig. 2, another parameter, the residual resistivity ρ_0, can be extracted. This property, that is otherwise difficult to obtained, can be easily found since it's just a scaling parameter used in the construction of Fig. 2. The residual resistivity ρ_0 is summarized in Table I.

The universal scaling of $\rho(T)$ in regions I and II [see Figs. 2(a), 2(b)] is a strong indication that in all high-T_c samples from the strongly underdoped to the nearly optimally doped samples, *the transport properties are dominated by the same underlying scattering mechanisms*. The only change that occurs when lowering the doping level is the energy scale for these processes. Since this scaling is in good agreement with the pseudo-spin-gap crossover temperature T^*, the dominant scattering mechanisms are probably of *magnetic origin*.

IV. HIGH FIELD MAGNETO RESISTIVITY

Figures 3(a)–3(c) and Figs. 3(d)–3(f) show, respectively, the $\rho_{ab}(H)$ curves measured at different temperatures for the $YBa_2Cu_3O_x$ films with $x=6.95$, 6.7, and 6.45 and for the

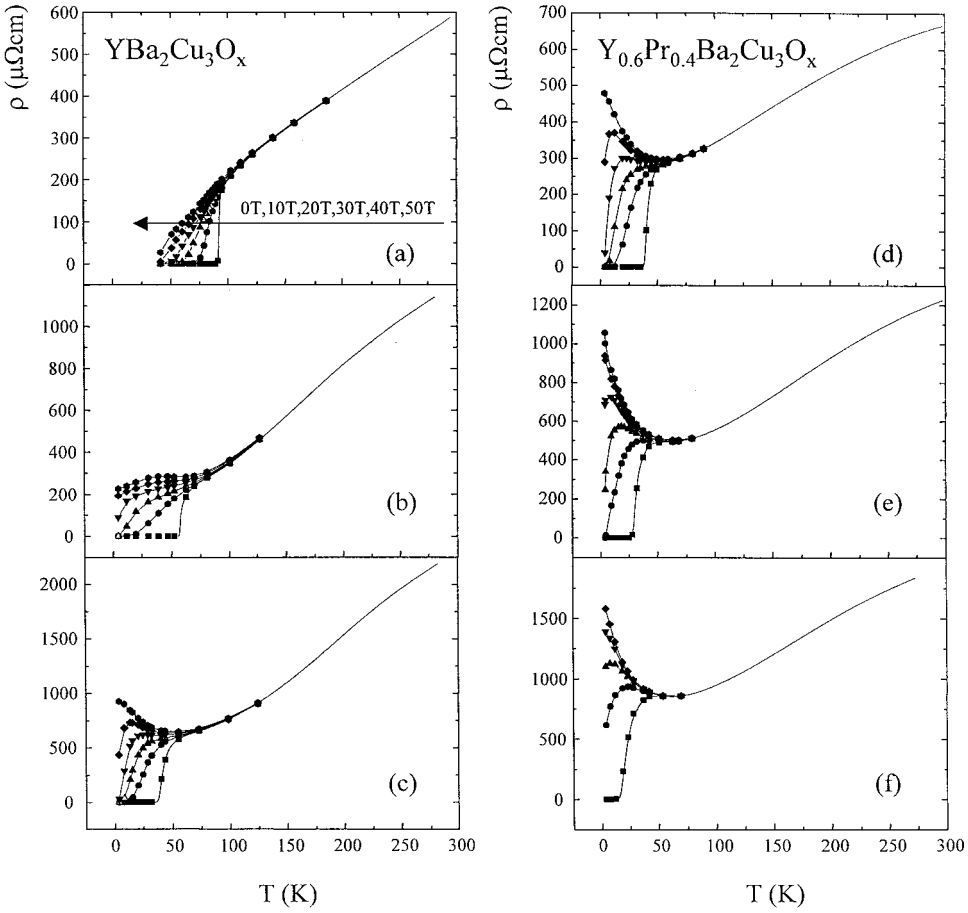

FIG. 4. Temperature dependencies of the in-plane resistivity $\rho_{ab}(T)$ for an epitaxial $(Y_{1-z}Pr_z)Ba_2Cu_3O_x$ thin films at different fields. The field H was applied $H\|c$ and the current $I\|ab$.

$Y_{0.6}Pr_{0.4}Ba_2Cu_3O_x$ films with $x=6.95$, 6.85, and 6.7. In the optimally doped case $YBa_2Cu_3O_{6.95}$ and above T_c, a small positive magnetoresistivity ($\sim H^2$) is present when sweeping the magnetic field up to 50 T. When lowering the temperature, even *just above* T_c a small low-field excess conductivity develops that is suppressed by high magnetic fields. Close to T_c, the $\rho(H)$ transition is narrow but broadens significantly at low temperatures. This indicates that the irreversibility field $H_{\rm irr}(T)$ and the second critical field $H_{c2}(T)$ are further separated from each other at low temperatures. From the $YBa_2Cu_3O_{6.7}$ data, presented in Fig. 3(b), similar observations can be made as for the optimally doped case. However, at the lowest temperatures the transition sharpens again. This indicates that the irreversibility line $H_{\rm irr}(T)$ and the second critical field $H_{c2}(T)$ come closer again after their initial separation at intermediate temperatures. The $\rho_{ab}(H)$ behavior for the $YBa_2Cu_3O_{6.45}$ sample, shown in Fig. 3(c), is very different from these at higher oxygen contents. At low temperatures, the high field $\rho_{ab}(H)$ data show a strong increase causing a *crossing* of the $\rho_{ab}(H)$ curves. The initial tendency of metallic $\rho_{ab}(T)$ behavior at high temperatures thus transforms into a more insulating behavior at low temperatures.

In the $(Y_{1-y}Pr_y)Ba_2Cu_3O_x$ system, the substitution of 40% of the Y atom by Pr already suppresses T_c to about 41 K and a further reduction of the charge carrier density by oxygen desorption induces an additional decrease of T_c. Figures 3(d), 3(e), and 3(f) present the $\rho_{ab}(H)$ curves at temperatures varying from $T \gg T_c$ down to 4.2 K for the $(Y_{0.6}Pr_{0.4})Ba_2Cu_3O_x$ films with $x=6.95$, 6.85, and 6.7. In all three cases an increasing $\rho_{ab}(50\,\mathrm{T})$ with lowering temperature is observed.

V. TEMPERATURE DEPENDENCE OF THE NORMAL-STATE RESISTIVITY BELOW T_c

On the basis of the high field $\rho_{ab}(H)$ curves in Fig. 3 for the $YBa_2Cu_3O_x$ and the $(Y_{0.6}Pr_{0.4})Ba_2Cu_3O_x$ thin films, it is possible to get information about the normal-state resistivity below T_c. It is however not clear *what criterion to take* in order to obtain a $\rho_{ab}(T)$ that is a true reflection of the normal-state properties. In this work, the choice was made to take the ρ_{ab} data at 50 T. The extent to which the 40-T data coincide with the 50-T data, is a good measure for the validity of this criterion. Figures 4(a)–4(e) present the $\rho_{ab}(T)$ curves for the $YBa_2Cu_3O_x$ films with $x=6.95$, 6.7, and 6.45. In the optimally doped case, the metallic behavior ($d\rho/dT > 0$) persists to below T_c and no saturation is present. Moreover, below 50 K the high magnetic fields do not destroy

superconductivity but simply broadens the $\rho_{ab}(T)$ transition. At lower oxygen content, the $\rho_{ab}(T)$ transition is broadened and the reduced energy scale (lower T_c and hence lower critical fields) causes the high field $\rho_{ab}(T)$ data to reflect the normal state more closely. At an oxygen content $x=6.45$, a plateau in $\rho_{ab}(T)$ transforms into an increasingly insulatorlike behavior ($d\rho/dT<0$) that diverges corresponding to the pronounced tendency of crossing $\rho_{ab}(H)$ curves in Fig. 3(c). This divergency is a strong indication that, even where superconductivity shows up, the ground state for $x\leqslant 6.7$ has an insulating or semiconducting nature.

Figures 4(d)–4(f) present the $\rho_{ab}(T)$ curves for the $(Y_{0.6}Pr_{0.4})Ba_2Cu_3O_x$ films with $x=6.95$, 6.85, and 6.7. Already in the fully oxygenated sample, the metallic behavior ($d\rho/dT>0$) above T_c transforms into an insulatinglike behavior ($d\rho/dT<0$) when suppressing the superconducting state and its fluctuations. This tendency is stronger in the oxygen deficient $x=6.85$ and $x=6.7$ samples. In these last two cases the normal state is attained easily and the low temperature state of insulatinglike (diverging) $\rho_{ab}(T)$ is clearly demonstrated in all the $(Y_{0.6}Pr_{0.4})Ba_2Cu_3O_x$ samples.

VI. SCALING OF THE NORMAL-STATE RESISTIVITY

In Fig. 5(a), the $\rho_{ab}(T)$ data, scaled by Δ, ρ_0, and ρ_Δ are given for the $YBa_2Cu_3O_x$ samples. For the optimally doped sample, the $\rho_{ab}(50\,\mathrm{T})$ curve follows the zero field $\rho_{ab}(T)$ accurately, until below $T/\Delta\sim 1$ the fields necessary to suppress superconductivity are higher than 50 T. Below $T/\Delta\sim 1$, the $\rho_{ab}(50\,\mathrm{T})$ curve starts to deviate from the zero field $\rho_{ab}(T)$ by showing the onset of the superconducting state. The $YBa_2Cu_3O_{6.7}$ sample demonstrates a clear tendency towards a saturating $\rho_{ab}(T)$ while lowering the temperature. The data for $YBa_2Cu_3O_{6.45}$, showing a diverging $\rho_{ab}(T)$ behavior at the lowest temperatures, seems to follow the universal curve to lower temperatures and a resistance minimum is observed at a temperature T_{MI} with $T_{MI}/\Delta\sim 0.25$. We can conclude that the resistivity versus temperature data for the $YBa_2Cu_3O_x$ system scale—in regions I and partially in region II—onto one universal curve. The samples with the highest oxygen content deviate noticeably from the universal behavior in region III. Most probably, the ground state is still masked by the incomplete destruction of superconductivity at $B=50\,\mathrm{T}$ for these nearly optimally doped films at low temperatures. In Fig. 5(b), the scaled $\rho_{ab}(T)$ is shown for the $(Y_{0.6}Pr_{0.4})Ba_2Cu_3O_x$ sample with $x=6.7$, 6.85, and 6.95. The high field data were added after scaling them with the same Δ, ρ_0, and ρ_Δ parameters employed for the zero-field scaling. In this case *a scaling was obtained for the diverging resistivity in region* III (apart from the scaling in regimès I and II). In the $(Y_{0.6}Pr_{0.4})Ba_2Cu_3O_x$ case, the resistance minimum was observed at $T/\Delta\sim 0.35$, somewhat higher than the ratio 0.25 found for $YBa_2Cu_3O_x$. The behavior of the resistivity in this region is dominated by the localization of charge carriers due to the disorder. It is rather surprising that the energy scale Δ describing the scattering process in the metallic regions I and II is also able to give a good description of these insulatorlike features in regime III. The $(Y_{0.6}Pr_{0.4})Ba_2Cu_3O_x$ samples demonstrate a high energy-scale Δ at fixed oxygen content (Table I) which, combined with the higher value $T/\Delta\sim 0.35$ for the resistance minimum, yields to a temperature T_{MI}, for the onset of localization, that lies significantly above the T_{MI} values for $YBa_2Cu_3O_x$ (with a lower Δ and $T/\Delta\sim 0.25$). The Pr substitution seems to enhance disorder considerably, resulting in a rather higher T_{MI}. Possible variations in $\rho(T)$ at low temperatures, caused by an additional disorder due to oxygen desorption, are made less clear by the high value of Δ, squeezing the low-temperature data together. On the other hand, since the insulatinglike behavior in the Pr-doped samples is much more pronounced than in the pure YBCO system, a real scaling seems to exist, and may have a link with the insulating nature nevertheless.

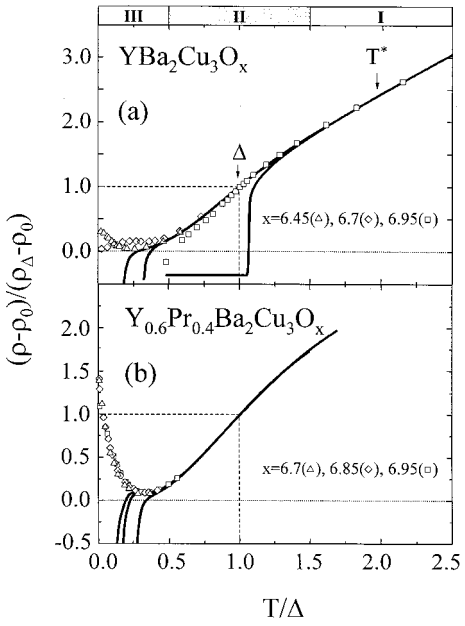

FIG. 5. Scaling of the zero field and 50 T $\rho(T)$ data for the $YBa_2Cu_3O_x$ thin films with $x=6.45$, 6.7, and $x=6.95$ (a) and for the $(Y_{0.6}Pr_{0.4})Ba_2Cu_3O_x$ thin films with $x=6.7$, $x=6.85$, and $x=6.95$ (b). The temperature is rescaled with a parameter Δ (an energy scalc) and the resistivity is given by $(\rho-\rho_0)/(\rho_\Delta-\rho_0)$ in which the residual resistivity ρ_0 is subtracted and ρ_Δ is the resistivity at $T=\Delta$. The three regions of different $\rho(T)$ behavior are indicated as well as the energy scale Δ and the crossover temperature T^*. We assume here that the parameters Δ, ρ_0, ρ_Δ are field independent (or at least only weakly field dependent).

VII. CONCLUSIONS

The temperature dependent resistivity of a set of $YBa_2Cu_3O_x$ and $(Y_{0.6}Pr_{0.4})Ba_2Cu_3O_x$ epitaxial thin films was measured in zero field and at very high pulsed magnetic fields. The zero-field data show that the samples are rather poor conductors having relatively low ratios $\rho_{290\,\mathrm{K}}/\rho_0$ [$\rho_{290\,\mathrm{K}}/\rho_0\sim 2.6$ to 12.2 for $YBa_2Cu_3O_x$ and $\rho_{290\,\mathrm{K}}/\rho_0\sim 2.5$ for $(Y_{0.6}Pr_{0.4})Ba_2Cu_3O_x$)] compared to pure normal metals where $\rho_{290\,\mathrm{K}}/\rho_0\sim 1000$. This agrees with previous findings on all superconducting high-T_c cuprates and indicates their

relative impurity. Furthermore, it was shown that the zero-field normal-state resistivity above T_c for various levels of hole doping—both for the $YBa_2Cu_3O_x$ and the $(Y_{0.6}Pr_{0.4})Ba_2Cu_3O_x$ members of the cuprate superconductors—can be scaled onto one single universal curve. An energy scale Δ, the resistivity ρ_Δ and the residual resistivity ρ_0 are used as scaling parameters. The universal curve exhibits a region (labeled I) of linear $\rho(T)$ at high temperatures $T>T^*$, a superlinear $\rho(T)$ at intermediate temperatures $T<T^*$ (region II) and a low temperature insulating $\rho(T)$ regime (labeled III) at $T<T_{MI}$. This low-temperature regime is masked by the presence of superconductivity below T_c. The distinct features in the temperature dependence of the metallic zero-field resistivity of $YBa_2Cu_3O_x$ and $(Y_{0.6}Pr_{0.4})Ba_2Cu_3O_x$ in regions I and II are universal for all the reported zero-field curves, the only difference is the temperature at which these features are seen. The existence of a universal $\rho(T)$ curve was interpreted as a strong indication that *the same mechanisms are dominating the scattering of the charge carriers*. These mechanisms then determine the doping dependent energy scale $\Delta(p)$. In order to gain access to the low-temperature $T<T_c$ part of the normal-state transport properties (regions II and III), experiments in high magnetic fields were performed. These experiments revealed the ground state of $YBa_2Cu_3O_x$ (for $x\leqslant 6.8$) and $(Y_{0.6}Pr_{0.4})Ba_2Cu_3O_x$ (for all levels of oxygen content) ultrathin film to be insulatinglike with the resistivity increasing as the temperature is lowered. Performing the same scaling analysis as in the zero-field case, it was shown that the high-field $\rho(T)$ data for region III—the insulating regime—do scale for the $(Y_{0.6}Pr_{0.4})Ba_2Cu_3O_x$ system. For the $YBa_2Cu_3O_x$ system, a magnetic field of 50 T is not sufficient to destroy superconductivity and its fluctuations below T_c. It was argued that if the scaling really exists, it should be linked with the insulating nature itself since the same energy scale Δ controls both the metallic (regions I and II) and the insulating (region III) part of the $\rho(T)$ curves.

ACKNOWLEDGMENTS

The Belgian IUAP, the Flemish GOA, and FWO programmes have supported this work.

[1] B. Wuyts, V. V. Moshchalkov, and Y. Bruynseraede, Phys. Rev. B **53**, 9418 (1996).
[2] Y. Ando, G. S. Boebinger, A. Passner, N. L. Wang, C. Geibel, and F. Steglich, Phys. Rev. Lett. **77**, 2065 (1996).
[3] Y. Ando, G. S. Boebinger, A. Passner, N. L. Wang, C. Geibel, F. Steglich, I. E. Trofimov, and F. F. Balakirev, Phys. Rev. B **56**, R8530 (1997).
[4] Y. Ando, G. S. Boebinger, A. Passner, N. L. Wang, C. Geibel, F. Steglich, T. Kimura, M. Okuya, J. Shimoyama, K. Kishio, K. Tamasaku, N. Ichikawa, and S. Uchida, Physica C **282-287**, 240 (1997).
[5] Y. Ando, G. S. Boebinger, A. Passner, T. Kimura, and K. Kishio, Phys. Rev. Lett. **75**, 4662 (1995).
[6] Y. Ando, G. S. Boebinger, A. Passner, R. J. Cava, T. Kimura, J. Shimoyama, and K. Kishio (unpublished).
[7] Y. Ando, G. S. Boebinger, A. Passner, K. Tamasaku, N. Ichikawa, S. Uchida, M. Okuya, T. Kimura, J. Shimoyama, and K. Kishio, J. Low Temp. Phys. **105**, 867 (1996).
[8] G. S. Boebinger, Y. Ando, A. Passner, T. Kimura, M. Okuya, J. Shimoyama, K. Kishio, K. Tamasaku, N. Ichikawa, and S. Uchida, Phys. Rev. Lett. **77**, 5417 (1996).
[9] B. Wuyts, Z. X. Gao, S. Libbrecht, M. Maenhoudt, E. Osquiguil, and Y. Bruynseraede, Physica C **203**, 235 (1992).
[10] E. Osquiguil, M. Maenhoudt, B. Wuyts, and Y. Bruynseraede, Appl. Phys. Lett. **60**, 1627 (1992).
[11] F. Herlach, L. Van Bockstal, M. van de Burgt, and G. Heremans, Physica B **155**, 61 (1989).
[12] F. Herlach, Ch. Agosta, R. Bogaerts, W. Boon, I. Deckers, A. De Keyser, N. Harrison, A. Lagutin, L. Li, L. Trappeniers, J. Vanacken, L. Van Bockstal, and Ann Van Esch, Physica B **216**, 161 (1996).
[13] C. C. Almasan, G. A. Levin, C. N. Jiang, T. Stein, D. A. Gajewski, S. H. Han, and M. B. Maple, Physica C **282-287**, 1129 (1997).
[14] B. Batlogg, H. Y. Hwang, H. Takagi, R. J. Cava, H. L. Kao, and J. Kwo, Physica C **235-240**, 130 (1994).
[15] C. N. Jiang, A. R. Baldwin, G. A. Levin, T. Stein, C. C. Almasan, D. A. Gajewski, S. H. Han, and M. B. Maple, Phys. Rev. B **55**, R3390 (1997).
[16] G. A. Levin, T. Stein, C. N. Jiang, C. C. Almasan, D. A. Gajewski, S. H. Han, and M. B. Maple, Physica C **282-287**, 1127 (1997).
[17] H. Takagi, B. Batlogg, H. L. Kao, J. Kwo, R. J. Cava, J. J. Krajewski, and W. F. Peck, Phys. Rev. Lett. **69**, 2975 (1992).
[18] V. V. Moshchalkov, Solid State Commun. **86**, 715 (1993).
[19] T. Timusk and B. Statt, Rep. Prog. Phys. **62**, 61 (1999).